Local density functional electronic structures of three stable icosahedral fullerenes

ARTICLE *in* THE JOURNAL OF PHYSICAL CHEMISTRY · OCTOBER 1991

Impact Factor: 2.78 · DOI: 10.1021/j100175a058

a distinctive and general feature of gas-phase aromatic substitution, occurs only in those cases where the electrophile fulfils certain requirements. Paramount among the latter seem to be the presence of H atoms carrying a substantial fraction of the positive charge, capable of establishing localized H bonds with the unshared electrons of the substituent, as well as a suitable geometry of the cation, allowing simultaneous interaction with the n-type and the π-type nucleophilic centers of the bidentate substrate, and finally the lack of steric hindrance to ortho substitution. All such features characterize to a comparable extent $i\text{-}C_3H_7^+$ and $(CH_3)_2F^+$, the two gaseous reactants that consistently give the highest extent of substitution ortho to groups containing unshared electron pairs.

Acknowledgment. We acknowledge the financial support of Italian National Research Council (CNR) and of Ministero della Ricerca Scientifica e Tecnologica (MURST).

Registry No. (Trifluoromethoxy)benzene, 456-55-3; ethylium, 14936-94-8; isopropylium, 19252-53-0; dimethylfluoronium, 64710-12-9; methyl nitrate conjugate monoacid, 99573-80-5.

Local Density Functional Electronic Structures of Three Stable Icosahedral Fullerenes

B. I. Dunlap,* D. W. Brenner, J. W. Mintmire, R. C. Mowrey, and C. T. White

Theoretical Chemistry Section, Code 6119, Naval Research Laboratory, Washington, D.C. 20375-5000
(Received: April 2, 1991)

Local density functional (LDF) electronic structures of icosahedral C_{60}, C_{180}, and C_{240} are compared. These molecules are remarkably similar, and nothing is found to suggest that the two larger molecules are less stable than C_{60}. Ionization potentials are calculated by using both the transition-state approximation and differences between self-consistent-field calculations. Comparing these with one-electron eigenvalues supports the interpretation of photoelectron line shapes using theoretical cross sections calculated from LDF one-electron states of these large, highly symmetric molecules.

1. Introduction

Icosahedral (I_h) C_{60} has been isolated in macroscopic quantities in several laboratories.[1-7] Buckminsterfullerene is the smallest in an infinite series of sp^2 carbon fullerenes[8] that are invariant under the 120 operations of I_h, the largest point group. The number of carbon atoms in the I_h fullerenes is given by the expression $20(i^2 + ij + j^2)$, for $j = 0$ or i.[9] Other values of j in this equation corresponds to fullerenes that are invariant only under the 60-operation point group, I, and thus not centrosymmetric. The clusters corresponding to $(i,j) = (1,0)$, C_{20}, and to $(i,j) = (2,0)$, C_{80}, are not closed-shell molecules in a Hückel molecular orbital treatment of the π electrons.[10] The Hückel closed-shell molecules considered in this work correspond to $(i,j) = (1,1)$, (3,0), and (2,2) and are C_{60}, C_{180}, and C_{240}, respectively.[10] In these molecules each atom is symmetry-equivalent to at least 59 others. Therefore, the strain associated with closing the molecules into a roughly spherical shape is distributed over at least 60 atoms. C_{180} and C_{240} have larger radial dimensions than C_{60}; therefore, the curvature away from perfectly planar sp^2 bonding with its three neighbors that each C_{180} and C_{240} carbon atom sees could be less than that of each C_{60} carbon atom. Group theory and Hückel theory suggest that C_{180} and C_{240} could be as stable as C_{60}, yet so far C_{180} and C_{240} have been neither seen as extraordinarily abundant clusters nor isolated chemically. If C_{180} and C_{240} are as stable as C_{60}, then perhaps new techniques can be found to synthesize them in quantity. If they can be synthesized they may be more stable than C_{60}.

Preliminary experimental data suggest that C_{60} is unstable to attack by molecular oxygen,[11-13] despite the fact that it has no defects or edges that might readily initiate oxidation. Perhaps larger fullerenes with less surface curvature would be more oxidatively stable and thus have greater applicability as precursors in materials science. A key to the discovery of current techniques for creating macroscopic amounts of C_{60} was infrared (IR)

TABLE I: Coordinates and Radial Distance from the Origin (R) of the Symmetry-Inequivalent C_{60}, C_{180}, and C_{240} Atoms[a]

	X, Å	Y, Å	Z, Å	R, Å
C_{60}	3.462	0.694	0.000	3.531
C_{180}	0.728	5.953	0.000	5.997
	3.430	5.021	0.000	6.081
	4.627	4.287	0.000	6.308
C_{240}	6.768	0.712	1.256	6.938
	6.921	1.381	0.000	7.057
	6.804	2.779	0.000	7.350

[a] The C_{60} coordinates are from LDF optimization, and the other sets of coordinates are optimized by using EP I.[20]

(1) Krätschmer, W.; Fostiropoulos, K.; Huffman, D. R. *Chem. Phys. Lett.* **1990**, *170*, 167.
(2) Krätschmer, W.; Lamb, L. D.; Fostiropolous, K.; Huffman, D. R. *Nature* **1990**, *347*, 354.
(3) Taylor, R.; Hare, J. P.; Abdul-Sada, A. K.; Kroto, H. W. *J. Chem. Soc., Chem. Commun.* **1990**, 1423.
(4) Johnson, R. D.; Meijer, G.; Bethune, D. S. *J. Am. Chem. Soc.* **1990**, *112*, 8983.
(5) Ajie, H.; Alvarez, M. M.; Anz, S. J.; Beck, R. D.; Diederich, F.; Fostiropoulos, K.; Huffman, D. R.; Krätschmer, W.; Rubin, Y.; Schriver, K. E.; Sensharma, D.; Whetten, R. L. *J. Phys. Chem.* **1990**, *94*, 8630.
(6) Haufler, R. E.; Conceicao, J.; Chibente, L. P. F.; Chai, Y.; Byrne, N. E.; Flanagan, S.; Haley, M. M.; O'Brien, S. C.; Pan, C.; Xiao, Z.; Billups, W. E.; Ciufolini, M. A.; Hauge, R. H.; Margrave, J. L.; Wilson, L. J.; Curl, R. F.; Smalley, R. E. *J. Phys. Chem.* **1990**, *94*, 8634.
(7) Hawkins, J. M.; Lewis, T. A.; Loren, S. D.; Meyer, A.; Heath, J. R.; Saykally, R. J. *J. Org. Chem.* **1990**, *55*, 6250.
(8) Kroto, H. W. *J. Chem. Soc., Faraday Trans.* **1990**, *86*, 2465.
(9) Fowler, P. W.; Cremona, J. E.; Steer, J. I. *Theor. Chim. Acta* **1988**, *73*, 1.
(10) Klein, D. J.; Seitz, W. A.; Schmalz, T. G. *Nature* **1986**, *323*, 703.
(11) Arbogast, J. W.; Darmanyan, A. P.; Foote, C. S.; Rubin, Y.; Diederich, F. N.; Alverez, M. M.; Anz, S. J.; Whetten, R. L. *J. Phys. Chem.* **1991**, *95*, 11.
(12) Haufler, R. E.; Chai, Y.; Chibante, L. P. F.; Conceicao, J.; Jin, C.; Wang, L.-S.; Maruyama, S.; Smalley, R. E. *Mater. Res. Soc. Symp. Proc.* **1991**, *206*, 627.
(13) Milliken, J.; Keller, T. M.; Baronavski, A. P.; McElvany, S. W.; Callahan, J. H.; Nelson, H. H. *Chem. Mater.* **1991**, *3*, 386.

spectroscopy.[1] The IR spectra of the larger fullerenes would necessarily be more complex. Successful synthesis of C_{180} and C_{240}, if possible, would likely require a battery of diagnostic spectroscopic methods. To aid in their possible synthesis and separation, we have computed the X-ray photoelectron spectroscopy (XPS) and ultraviolet photoelectron spectroscopy (UPS) local density functional (LDF) spectra of these molecules.

2. LDF Basis Sets and Molecular Geometries

The LDF used herein is the Perdew–Zunger[14] (PZ) fit that interpolates between the essentially exact Ceperley–Alder[15] free-electron gas calculations in the completely ferromagnetic and completely paramagnetic limits. The starting linear combination of Gaussian type orbital (LCGTO) basis set, an 11s/7p basis,[16] was augmented with a d exponent of 0.6 bohr^{-2}.[17] The orbital basis set was contracted 2,3/1,2/0,1, where for each angular momentum the numbers of contracted atomic functions and uncontracted diffuse Gaussians are separated by a comma. The 11s functions were scaled by 2 and $^2/_3$ to generate the spherically symmetric parts of the charge density and exchange-correlation fitting basis, respectively.[18] To fit angular variations around each atom, five p and five d fitting exponents were used with exponents 0.25, 0.37, 0.7, 2.0, and 5.0 bohr^{-2}. The bond-centered exponents were 1.0 and 0.33 bohr^{-2} for the charge density and exchange-correlation basis sets, respectively. This carbon atom basis was used in studies of C_{60}, $C_{60}H_{60}$, and $C_{60}F_{60}$.[19] For I_h C_{240}, the size of this orbital basis set is 4560 and the dimension of the largest secular matrix is 199.

Table I gives the coordinates of the symmetry-inequivalent atoms of the molecules used in this study. Each of the atoms listed in this table is symmetry-equivalent to 59 others except the first atom listed for C_{240}, which represents a 120-atom set as indicated by its nonzero z coordinate. The coordinates refer to a system in which the 12 5-fold axes point in the four $\{\pm\alpha,\pm\beta,0\}$ directions, where

$$\alpha = \left[\left(1 + \frac{1}{\sqrt{5}}\right)/2\right]^{1/2} \qquad \beta = \left[\left(1 - \frac{1}{\sqrt{5}}\right)/2\right]^{1/2} \quad (1)$$

and the eight other directions obtained by the two cyclic permutations of these Cartesian coordinates. The C_{60} coordinates were optimized by using the PZ LDF.[19] The other two molecules were optimized by using empirical potential (EP) I of ref 20. The LDF bond distances for C_{60} are 1.39 and 1.45 Å. The EP I bond distances for C_{60} are 1.42 and 1.45 Å. The EP I short bond distance is essentially the same as the in-plane bond distance of graphite as a consequence of the method of parametrization.[20] The all-electron total LDF energy difference between the LDF and EP I C_{60} geometries is 0.58 eV. The symmetry-inequivalent nearest-neighbor bond distances in C_{180} are 1.40, 1.43, 1.43, and 1.46 Å, and for C_{240} are 1.39, 1.41, 1.44, 1.45, and 1.47 Å. The LDF one-electron eigenvalues in the vicinity of the highest occupied molecular orbital (HOMO) and lowest unoccupied molecular orbital (LUMO) for these three molecules are given in Table II. In this table the HOMO–LUMO gap is indicated by a vertical space. Relative to the eigenvalues quoted for C_{60} in the table, the C_{60} eigenvalues at the EP I geometry are lower by −0.09 to −0.21 eV for the unoccupied levels and vary from +0.07 to −0.06 eV for the occupied levels. (The LDF HOMO–LUMO gap at the EP I geometry is reduced by 0.02 eV). The ordering of none of the levels is altered. Based on this level of agreement, no LDF optimizations of the geometries of C_{180} and C_{240} have been performed at this time. The average radial distances to each carbon atom and standard deviations for C_{180} and C_{240} are 6.129 ± 0.075 and 7.070 ± 0.084 Å, respectively. The LDF radial distance of C_{60} is 3.531 Å. Doubling that distance yields 7.062 Å, which is very close to the average radial distance of C_{240}, which must therefore have almost exactly 4 times the surface area. While all three molecules are constrained to be close to spherical because of their I_h point-group symmetry, C_{60} is somewhat more spherical than C_{180} and C_{180} is somewhat more spherical than C_{240}.

TABLE II: LDF One-Electron Symmetry and Eigenvalues (in eV) about the HOMO–LUMO Gap (Indicated by a Vertical Space) in C_{60}, C_{180}, and C_{240}

C_{60}		C_{180}		C_{240}	
7 g_g	−0.11	29 h_g	−2.57	25 g_u	−2.85
7 h_u	−0.56	19 g_u	−2.81	27 h_u	−2.95
11 h_g	−2.07	28 h_g	−3.10	11 a_g	−3.08
7 t_{2u}	−2.25	18 t_{2u}	−3.12	35 h_g	−3.38
3 t_{1g}	−3.15	10 t_{1g}	−4.11	15 t_{1g}	−4.07
7 t_{1u}	−4.26	18 t_{1u}	−4.46	23 t_{1u}	−4.37
6 h_u	−5.94	19 h_u	−5.84	26 h_u	−5.54
6 g_g	−7.12	27 h_g	−6.12	34 h_g	−5.95
10 h_g	−7.24	18 g_u	−6.16	24 g_g	−6.04
5 h_u	−8.78	18 g_g	−6.36	14 t_{2g}	−6.56
6 g_u	−8.83	9 t_{2g}	−6.93	14 t_{1g}	−6.62
9 h_g	−9.09	26 h_g	−7.05	24 g_u	−6.66
6 t_{2u}	−9.38	17 g_u	−7.58	25 h_u	−6.87
5 g_u	−10.10	18 h_u	−7.59	22 t_{1u}	−7.02
2 t_{2g}	−10.58	17 t_{2u}	−7.66	23 g_u	−7.06
8 h_g	−10.70	17 t_{1u}	−7.90	22 t_{2u}	−7.20
5 g_g	−10.85	25 h_g	−8.23	33 h_g	−7.69
7 h_g	−11.26	17 h_u	−8.27	23 g_g	−7.71
4 g_u	−11.75	17 g_g	−8.54	13 t_{2g}	−7.79
6 t_{1u}	−11.84	9 t_{1g}	−8.65	32 h_g	−7.98
4 a_g	−12.44	24 h_g	−8.88	24 h_u	−8.14
5 t_{2u}	−12.47	16 g_g	−8.99	31 h_g	−8.21
5 t_{1u}	−13.05	8 t_{2g}	−9.09	22 g_u	−8.54
4 h_u	−13.25	16 g_u	−9.15	21 t_{2u}	−8.68

3. Ionization Potentials and Electron Affinities

The LDF electronic structure of C_{60} is $2t_{1g}4a_g6t_{1u}2t_{2g}6t_{2u}6g_u10h_g6g_g6h_u$, of C_{180} is $1a_u9a_g9t_{1g}17t_{1u}17t_{2u}9t_{2g}18g_g18g_u27h_g19h_u$, and of C_{240} is $2a_u10a_g22t_{2u}22t_{1u}24g_u14t_{1g}14t_{2g}24g_g34h_g26h_u$. The LDF binding energy per atom of C_{60}, C_{180}, and C_{240} is 196.2 (LDF geometry, 196.5 EP I geometry), 201.1, and 202.0 kcal/mol, respectively. LDF optimization of the geometry of C_{180} and C_{240} would increase slightly the these last two numbers; thus, per carbon atom both C_{180} and C_{240} are significantly more stable than C_{60}. the experimental enthalpy of formation (0 K) of a carbon atom from graphite is 170.0 kcal/mol.[21] The fact that the LDF binding energies of the I_h fullerenes are greater than the experimental enthalpy of formation of atomic carbon is simply another manifestation of the fact that recent LDFs overbind most molecules.[18] The remainder of this work considers only relative energy differences, which are expected to be quite reliable.[19]

The LDF one-electron eigenvalue spectra of Table II are extended from 0 eV to the bottom of the valence band of these three fullerenes in Figure 1. These spectra are remarkably similar. The valence bandwidths of C_{60}, C_{180}, and C_{240} are 18.59, 18.36, and 18.61 eV, respectively. All three molecules have h_u HOMOs and t_{1u} LUMOs. Furthermore, the second LUMO of these three molecules is t_{1g}, and three of the first four HOMOs of each of these molecules are h_u, h_g, and g_g. The H and G irreducible representations, which have dimensions 4 and 5, respectively, of I and I_h are the largest irreducible representations of these groups. The HOMO–LUMO excitations in these molecules are electric dipole forbidden. The HOMO–LUMO gaps of C_{60}, C_{180}, and C_{240} are 1.68, 1.38, and 1.16 eV, respectively.

(14) Perdew, J. P.; Zunger, A. *Phys. Rev. B* **1981**, *23*, 5948.
(15) Ceperley, D. M.; Alder, B. J. *Phys. Rev. Lett.* **1980**, *45*, 566.
(16) van Duijneveldt, F. B. *IBM Res. Rep.* **1971**, *RJ945*.
(17) Huzinaga, S., Ed. *Gaussian Basis Sets for Molecular Calculations*; Elsevier: Amsterdam, 1984.
(18) Dunlap, B. I.; Connolly, J. W. D.; Sabin, J. R. *J. Chem. Phys.* **1979**, *71*, 3396, 4993.
(19) Dunlap, B. I.; Brenner, D. W.; Mintmire, J. W.; Mowrey, R. C.; White, C. T. *J. Phys. Chem.* **1991**, *95*, 5763.
(20) Brenner, D. W. *Phys. Rev. B* **1990**, *42*, 9458.
(21) Chase, Jr., M. W.; Davies, C. A.; Downey, Jr., J. R.; Frurip, D. J.; McDonald, R. A.; Syverud, A. N. *J. Phys. Chem. Ref. Data* **1985**, *14* (Suppl. 1).

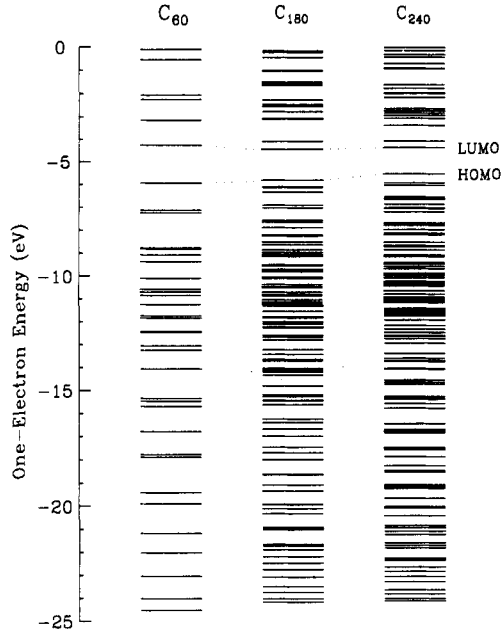

Figure 1. LDF one-electron energy levels of C_{60}, C_{180}, and C_{240}. All are closed-shell, have a large HOMO–LUMO gaps, and have electric dipole forbidden HOMO–LUMO excitations.

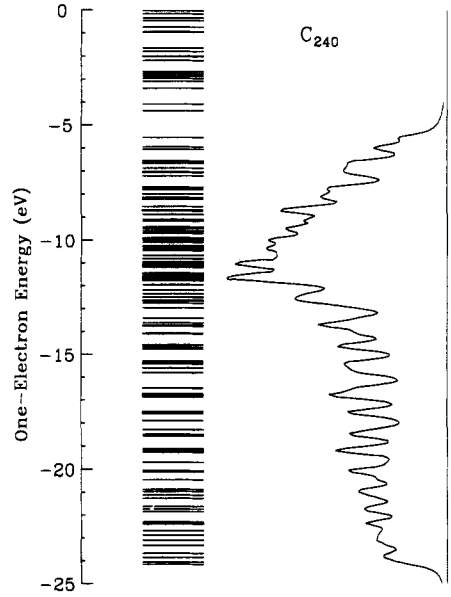

Figure 2. C_{240} LDF one-electron energy levels (left) and corresponding density of states obtained by Lorentz broadening these levels by 0.2 eV full width at half-maximum.

Large fullerenes contain a fixed number of carbon atoms (60 for isolated pentagons) at the vertices of the 12 pentagons necessary for closure. Therefore, as they become larger, an increasing percentage of carbon atoms are in an essentially graphitic environment, i.e., surrounded by three hexagons formed by neighboring carbon atoms. To compare to band structure density of states for graphite, we have Lorentz broadened the occupied valence levels of C_{240} by 0.2 eV in Figure 2. The width of the valence density of states for graphite obtained by using the Xα LDF is 20.7 eV[22,23] in contrast to 18.6 eV for C_{240} using the PZ LDF. Neglecting the rapid variations for small changes in energy, both densities of states increase roughly linearly from the Fermi energy (band structure) and HOMO (C_{240}) to peaks at 8 and 6 eV, respectively, greater binding. For binding energies that are at least 2 eV greater still, both densities of states are flatter from peak to peak.

(22) Painter, G. S.; Ellis, D. E. *Phys. Rev. B* **1970**, *1*, 4747.
(23) Willis, R. F.; Fitton, B.; Painter, G. S. *Phys. Rev. B* **1974**, *9*, 1926.

TABLE III: LDF IPs Computed Using the One-Electron Eigenvalues (ϵ) and the Transition-State (TS) Method and Computed Directly (ΔSCF)[a]

state	ϵ	TS	ΔSCF
		C_{60}	
6 h_u	5.94 (0.00)	7.49 (0.00)	7.60 (0.00)
6 g_g	7.12 (1.18)	8.68 (1.19)	8.78 (1.18)
10 h_g	7.24 (0.12)	8.79 (0.11)	8.88 (0.10)
5 h_u	8.78 (1.54)	10.40 (1.61)	10.48 (1.60)
6 g_u	8.83 (0.05)	10.38 (−0.02)	10.47 (−0.01)
		C_{180}	
19 h_u	5.84 (0.00)		6.91 (0.00)
27 h_g	6.12 (0.28)		7.19 (0.28)
18 g_u	6.16 (0.04)		7.24 (0.05)
18 g_g	6.36 (0.20)		7.43 (0.19)
		C_{240}	
26 h_u	5.54 (0.00)		6.52 (0.00)
34 h_g	5.95 (0.41)		6.93 (0.41)
24 g_g	6.04 (0.09)		7.03 (0.10)
14 t_{2g}	6.56 (0.52)		7.55 (0.52)

[a] The IPs and parenthetically the separation from the next higher IP are given in eV.

The LDF one-electron eigenvalues provide a zeroth-order estimate of the ionization potentials (IPs) and electron affinities (EAs) of these molecules. Precise LDF IPs and EAs are given by the difference in total energies between two different self-consistent-field (ΔSCF) calculations in which the one-electron orbitals are occupied appropriate to the initial and final states. A third way to compute LDF IPs and electron IAs is to use the transition-state (TS) method. This latter method is based on the fact that the LDF eigenvalues are exact derivatives of the total energy with respect to occupation number:[24,25] The IPs and EAs are then given by the eigenvalues of the relevant orbital occupied by half an electron; i.e., the occupation numbers used in the calculation are the average of those of the initial and final states. The TS method is rather accurate because the electron–electron interaction is to a good approximation a second-order polynomial of the one-electron occupation numbers for small relative changes in the vector of occupation numbers. Table III gives several IPs for C_{60} obtained by using these three methods and for C_{180} and C_{240} using only the eigenvalue method (ϵ) and ΔSCF methods.

To a first approximation the C_{60} LDF IPs, determined simply by equating them to the negative of the various occupied one-electron eigenvalues of the neutral state calculation, must be increased by 1.67 eV to get the ΔSCF values for the five states of Table III. Similarly, the TS IPs must be increased by 0.10 eV to get the ΔSCF values. All other effects, including the reversal of the $5h_u$ and $6g_u$ IPs by using eigenvalues rather than computing TS or ΔSCF IPs, are almost an order of magnitude smaller ($\pm$0.03 eV using the eigenvalue method and $\pm$0.01 eV using the TS method) than these first-order effects.

The ΔSCF C_{60} IPs of Table III are uniformly 1.1 eV larger than those of Table II of ref 26 (the last entry in that table should be for $6g_u$, not $6g_g$) that were computed by using the same methods, but slightly smaller basis sets. This difference is caused by the fact that using variational weights in fitting the exchange-correlation potential[27] permits the use of very diffuse fitting functions without introducing numerical problems.[28] Apparently the tails of the LDF potentials are quite important in computing IPs for these large systems. The experimental first IP of C_{60} is 7.6 eV.[29,30] Our first IP is also in agreement with a TS first IP of 7.8 eV computed by using a slightly different LDF.[31]

(24) Slater, J. C.; Johnson, K. H. *Phys. Rev. B* **1972**, *5*, 844.
(25) Janak, J. F. *Phys. Rev. B* **1978**, *18*, 7165.
(26) Dunlap, B. I. *Int. J. Quantum Chem. Symp.* **1988**, *22*, 257.
(27) Dunlap, B. I.; Cook, M. *Int. J. Quantum Chem.* **1986**, *29*, 767.
(28) Dunlap, B. I.; Mei, W. N. *J. Chem. Phys.* **1983**, *78*, 4997.
(29) Lichtenberger, D. L.; Nebesny, K. W.; Ray, C. D.; Huffman, D. R.; Lamb, L. D. *Chem. Phys. Lett.* **1991**, *176*, 203.
(30) Zimmerman, J. A.; Eyler, J. R.; Bach, S. B. H.; McElvany, S. W. *J. Chem. Phys.* **1991**, *94*, 3556.

TABLE IV: LDF EAs Computed Using the One-Electron Eigenvalues (ϵ) and the Transition-State (TS) Method and Computed Directly (ΔSCF)[a]

state	ϵ	TS	ΔSCF
		C_{60}	
$3\ t_{1g}$	3.15 (1.11)	1.61 (1.11)	1.71 (1.11)
$7\ t_{1u}$	4.26 (0.00)	2.72 (0.00)	2.82 (0.00)
		C_{180}	
$10\ t_{1g}$	4.11 (0.35)		3.21 (0.35)
$18\ t_{1u}$	4.46 (0.00)		3.56 (0.00)
		C_{240}	
$15\ t_{1g}$	4.07 (0.30)		3.31 (0.30)
$23\ t_{1u}$	4.37 (0.00)		3.61 (0.00)

[a] The EAs and parenthetically the separation from the next lower EA are given in eV.

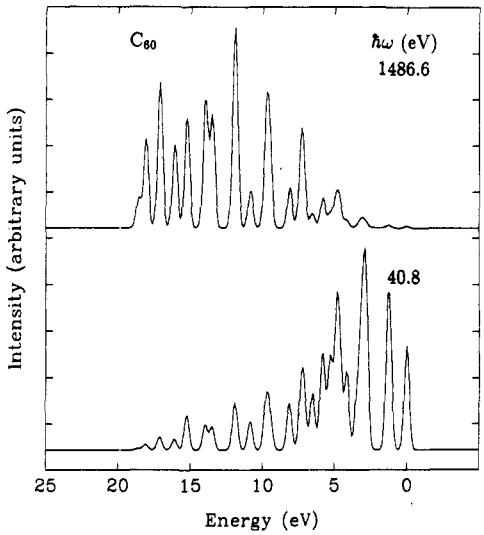

Figure 3. Calculated photoelectron spectra for C_{60} Gaussian broadened by 0.4 eV full width at half-maximum.

For the two larger systems the eigenvalue IPs must be shifted less, 1.07 eV for C_{180} and 0.98 eV for C_{240}, to yield the ΔSCF values of Table III. Furthermore, the errors in simply shifting the eigenvalue IPs of these larger molecules are significantly smaller, less than ±0.01 eV.

Table IV is similar to Table III but for the two first EAs. To a first approximation, the negatives of the various unoccupied one-electron eigenvalues of ground-state calculation are an estimate of the electron affinities. Only two states of each molecule are considered for EA computation in Table IV because the Gaussian basis sets used in these LDF calculations did not include a sufficient number of diffuse Gaussians to approach the continuum limit very closely. Nevertheless, we conclude downward shifts of the eigenvalue EAs of 1.44, 0.90, and 0.76 eV reproduce the ΔSCF EAs of C_{60}, C_{180}, and C_{240}, respectively. For C_{60} the TS EAs must be shifted downward by 0.10 eV.

4. Photoelectron Spectra

We have shown that if the outgoing electron is described by a plane wave, the initial and final bound wave functions are single determinants of unrelaxed initial-state orbitals, and the final-state energies are given by the appropriate initial-state eigenvalue, then the photoelectron cross sections are particularly simple to compute because they are related to the Fourier transform of the one-electron orbitals.[32-34] Furthermore, these assumptions together

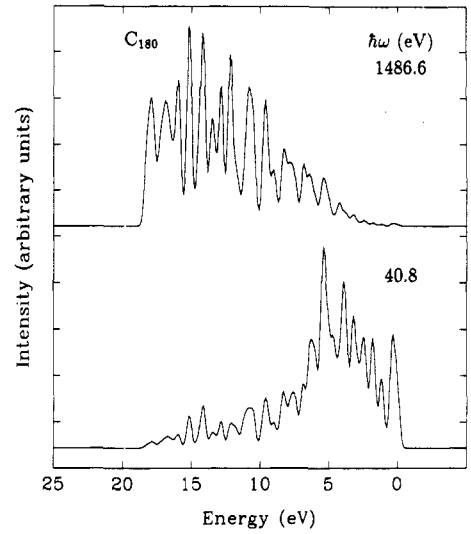

Figure 4. Calculated photoelectron spectra for C_{180} Gaussian broadened by 0.4 eV full width at half-maximum.

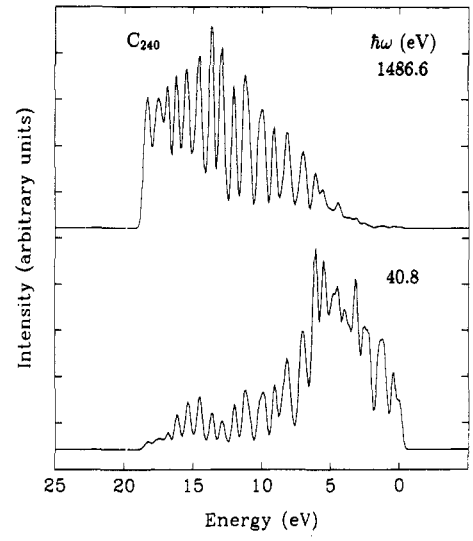

Figure 5. Calculated photoelectron spectra for C_{240} Gaussian broadened by 0.4 eV full width at half-maximum.

with the appropriate shift in the photon energy that is necessary to approximately map the one-electron eigenvalues into the final-state energies give excellent agreement with experiment.[32-34] As was shown above, the appropriate shifts for C_{60}, C_{180}, and C_{240} are 1.67, 1.07, and 0.98 eV, respectively.

Figures 3–5 give the calculated photoelectron spectra of C_{60}, C_{180}, and C_{240} Gaussian broadened by 0.4 eV. At this resolution all three molecules are clearly distinct, at both XPS energies, e.g., using Al K_α radiation at 1486.6 eV, and UPS energies, e.g., using the He II line at 40.8 eV. The former energy has greater cross section for predominantly s-like states deep in valence manifold of states, and the latter emphasizes the predominantly p-like states at the top of the valence manifold of states. For C_{60} these spectra are in excellent agreement[34] with recent experimental data.[29,35]

In going from C_{60} to the two larger fullerenes these spectra necessarily contain more peaks, but the variation between adjacent peak heights is much reduced in going to each of the larger fullerenes. Adjacent peak height variations are still large enough in the upper half of Figure 4 that XPS could still be a useful diagnostic in C_{180} production. The peak-to-peak variations in the C_{240} spectra are much smoother. With much greater broadening the C_{240} spectra would resemble the six-peak structure of the intermediate energy synchrotron photoemission spectra of graphite

(31) Rosén, A.; Wästberg, B. *J. Chem. Phys.* **1989**, *90*, 2525.
(32) Mintmire, J. W.; White, C. T. *Int. J. Quantum Chem. Symp.* **1983**, *17*, 609.
(33) Mintmire, J. W.; Kutzler, F. W.; White, C. T. *Phys. Rev. B* **1987**, *36*, 3312.
(34) Mintmire, J. W.; Dunlap, B. I.; Brenner, D. W.; Mowrey, R. C.; White, C. T. *Phys. Rev. B* **1991**, *43*, 14281.
(35) Weaver, J. H.; Martins, J. L.; Komeda, T.; Chen, Y.; Ohno, T. R.; Kroll, G. H.; Troullier, N.; Haufler, R. E.; Smalley, R. E. *Phys. Rev. Lett.* **1991**, *66*, 1741.

at 122 eV, which corresponds quite well to the graphite LDF density of states.[36]

5. Conclusions

LDF atomization energies are significantly greater for icosahedral C_{180} and C_{240} than for icosahedral C_{60}. Both of these larger fullerenes have only slightly smaller HOMO–LUMO gaps and ionization potentials than C_{60}. C_{60} has an electron affinity that is smaller than the electron affinities of C_{180} and C_{240} by 0.7 and 0.8 eV, respectively. Thus, we see no energetic barrier to the creation of these two larger I_h fullerenes.

If these two larger molecules cannot be made in significant quantities by using methods similiar to those used to isolate C_{60}, C_{70}, and C_{84},[1-7] despite the fact that laser vaporization sources can currently generate carbon clusters in this larger mass range, then it is likely that the isomerization energy associated with moving one of the 12 pentagons of carbon atoms around on the surface of fullerenes in at least the C_{180} to C_{240} size range is quite low. If they can be made in quantity, then our photoelectron spectra should be a useful diagnostic.

Note: After we submitted this paper, MNDO calculations of the vibrational spectra of these three (and other) fullerenes[37] have appeared and have been brought to our attention.

Acknowledgment. These calculations were made using a grant of CRAY X-MP computer time from the U.S. Naval Research Laboratory. This work was supportd in part by the Office of Naval Research (ONR) through the Naval Research Laboratory and through the ONR Chemistry Division Contract N00014-91-WX-24154.

(36) Bianconi, A.; Hagström, S. B. M.; Bachrach, R. Z. *Phys. Rev. B* **1977**, *16*, 5543.

(37) Bakowies, D.; Thiel, W. *J. Am. Chem. Soc.* **1991**, *113*, 3704; *Chem. Phys.* **1991**, *151*, 309.

Temperature Dependence of the Kinetics of the Reaction BO + O_2

C. T. Stanton,† Nancy L. Garland, and H. H. Nelson*

Chemistry Division/Code 6110, Naval Research Laboratory, Washington, DC 20375-5000
(Received: April 2, 1991; In Final Form: June 19, 1991)

The temperature and pressure dependence of the rate constant for the reaction of BO + O_2 is investigated in a high-temperature flow reactor. BO is generated by photolysis of $BCl_2(OCH_3)$ and detected by laser-induced fluorescence. Rate constants are obtained by monitoring the decay of the BO signal as a function of added O_2 pressure. The rate constant at room temperature is $(1.94 \pm 0.18) \times 10^{-11}$ cm^3 s^{-1} and is found to be pressure independent between 20 and 200 Torr. The temperature dependence of the rate constant between 300 and 1000 K can be represented by the Arrhenius expression $k(T) = (7.0 \pm 0.6) \times 10^{-12}$ cm^3 s^{-1} exp[$(0.51 \pm 0.08$ kcal mol^{-1})/RT]. A mechanism involving formation of a BO_3 adduct with subsequent decomposition to BO_2 + O is proposed to account for the observed negative temperature dependence.

Introduction

There has been a recent resurgence of interest in the chemical reactions of small boron-containing radicals for several reasons. First, boron compounds, especially hydrides, oxides, and oxyhydrides, are extremely attractive systems for theoretical study because they have a small number of valence electrons. Calculations of heats of formation, reaction rate constants, and dimerization energies of boron species have been reported recently.[1-5] Second, there is a practical interest in the combustion of boron and boron-doped hydrocarbon fuels and propellants due to the potential for large energy release on combustion of these systems. The highest gravimetric and volumetric exothermicities are available from the combustion of elemental boron; however, this process is hampered by the presence of a boron oxide coating on the boron particles which inhibits oxygen transport to the elemental boron. One solution to this problem is to burn the boron as an additive in a system where there are sufficient radicals present at lower temperatures to attack the oxide layer or in which the temperature is high enough for the oxide coating to vaporize. This is the situation that may be found, for example, in the combustion of boron-doped hydrocarbon fuels. A homogeneous combustion model for such a system of boron doped in hydrocarbon fuels has recently been published.[6]

The oxidation of boron proceeds through the sequence

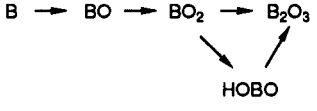

(1)

One of the key reactions in this sequence is the reaction of BO with molecular oxygen

$$BO + O_2 \rightarrow BO_2 + O \qquad (2)$$

Reliable modeling of boron combustion requires an accurate characterization of the temperature and pressure dependence of the rate constants for this and other elementary reactions which lead from B to B_2O_3.

There have been two reports of the room temperature rate constant for reaction 2.[7,8] Llewellyn, Fontijn, and Clyne[7] investigated the feasibility of using flow tube techniques to study reactions of boron oxide radicals. BO for this study was generated by the reaction of BCl_3 with N and O atoms produced in a microwave discharge. This method was used to avoid the problem of dimer (B_2O_2) formation[10] which plagued other BO production techniques. However, it resulted in low fluxes of BO and cor-

†ONT/NRL Postdoctoral Research Associate. Present address: Code R13, Naval Surface Warfare Center, Silver Spring, MD 20903-5000.

(1) Page, M. *J. Phys. Chem.* **1989**, *93*, 3639.
(2) Page, M.; Adams, G.; Binkley, J. S.; Melius, C. F. *J. Phys. Chem.* **1987**, *91*, 2675.
(3) Curtiss, L. A.; Pople, J. A. *J. Chem. Phys.* **1988**, *89*, 614.
(4) Dewar, M. J. S.; Jie, C.; Zoebisch, E. G. *Organometallics* **1988**, *7*, 513.
(5) Harrison, J. A.; Maclagan, R. G. A. R. *Chem. Phys. Lett.* **1988**, *146*, 243.
(6) Yetter, R. A.; Rabitz, H.; Dryer, F. L.; Brown, R. C.; Kolb, C. E. *Combust. Flame* **1991**, *83*, 43.
(7) Llewellyn, I. P.; Fontijn, A.; Clyne, M. A. A. *Chem. Phys. Lett.* **1981**, *84*, 504.
(8) Oldenborg, R. C.; Baughcum, S. L.; Winn, K. R. Submitted to *J. Phys. Chem.*
(9) Oldenborg, R. C.; Baughcum, S. L. *Advances in Laser Science I*; AIP Conference Proceedings 146; Stwalley, W. C., Lapp, M., Eds.; AIP: New York, 1986; p 562.
(10) Scheer, M. D. *J. Phys. Chem.* **1958**, *62*, 490.

0022-3654/91/2095-8741$02.50/0